

## TRAP1 Regulates Autophagy in Lung Cancer Cells

Ines A. Barbosa<sup>1</sup>, Ignacio Vega-Naredo<sup>1,2</sup>, Rute Loureiro<sup>1</sup>, Ana F. Branco<sup>1</sup>, Rita Garcia<sup>1</sup>,  
Patricia M. Scott<sup>3</sup>, Paulo J. Oliveira<sup>1\*</sup>

<sup>1</sup>*CNC-Center for Neuroscience and Cell Biology, University of Coimbra, UC Biotech Building, Lot 8A, Biocant Park, 3060-197 Cantanhede, Portugal*

<sup>2</sup>*Department of Morphology and Cell Biology, University of Oviedo, 33006 Oviedo, Spain.*

<sup>3</sup>*Department of Biomedical Sciences, University of Minnesota Medical School, Duluth Campus, MN, USA*

**\*Address correspondence to:**

CNC - Center for Neuroscience and Cell Biology

UC Biotech Building, University of Coimbra Lot 8A, Biocant Park, 3060-197 Cantanhede

PORTUGAL

phone: +351-231-249-195, fax: +351-231-249-179

email: pauloliv@cnc.uc.pt

**Running title: TRAP-1 regulates autophagy and mitochondrial function in A549 cells**

**Keywords:** TRAP1; lung cancer; macroautophagy; apoptosis; cathepsin-B; autophagy

Word count: 3507 words, 5 images

1  
2  
3  
4  
5 ABSTRACT

6 Background: Expression of TRAP1, a member of the HSP90 chaperone family, has been  
7 implicated in tumor protective effects, based on differential mitochondrial localization and  
8 function.  
9

10  
11  
12 Design: This work was designed to provide new insights on the pathways involved in  
13 TRAP1-provided cytoprotection on NSCLC. For this, TRAP1-depleted A549 human NSCLC  
14 cells and MRC-5 normal lung fibroblasts were produced using a siRNA approach and main  
15 cellular quality control mechanisms were investigated.  
16  
17

18  
19  
20 Results: TRAP1-depleted A549 cells displayed decreased cell viability likely due to impaired  
21 mitochondrial function including decreased ATP/AMP ratio, oxygen consumption and  
22 membrane potential, as well as increased apoptotic indicators. Furthermore, the negative  
23 impact of TRAP1 depletion on mitochondrial function was not observed in normal MRC-5  
24 lung cells, which might be due to the differential intracellular localization of the chaperone in  
25 tumor versus normal cells. Additionally, A549 TRAP1-depleted cells showed increased  
26 autophagic flux. Functionally, autophagy inhibition resulted in decreased cell viability in both  
27 TRAP1-expressing and TRAP1-depleted tumor cells with minor effects on MRC-5 cells.  
28 Conversely, autophagy stimulation decreased cell viability of both A549 and MRC-5 TRAP1-  
29 expressing cells while in A549 TRAP1-depleted cells, increased autophagy augmented  
30 viability.  
31  
32

33  
34  
35 Conclusions: Our results show that even though TRAP1 depletion affects both normal MRC-  
36 5 and tumor A549 cell proliferation, inhibition of autophagy *per se* led to a decrease in tumor  
37 cell mass, while having a reduced effect on the normal cell line. The strategy of targeting  
38 TRAP1 in NSCLC shows future potential therapeutic applications.  
39  
40  
41  
42  
43  
44  
45  
46  
47  
48  
49  
50  
51  
52  
53  
54  
55  
56  
57  
58  
59  
60

## INTRODUCTION

The chaperone gene Tumor Necrosis Factor Receptor-Associated Protein 1, TRAP1, is a member of the HSP90 family with predominantly mitochondrial localization, whose cytoprotective role has been widely documented [1-4]. Several studies suggest that TRAP1 preserves cellular function by protecting mitochondrial function by limiting the effects of oxidative stress by decreasing reactive oxygen species (ROS)-mediated oxidation [5] or by attenuating ROS production [6, 7], and by preserving mitochondrial membrane potential by limiting mitochondrial permeability transition pore (mPTP) opening through its interaction with HSP90 and cyclophilin D (CypD) [3, 8]. Recent studies identify additional cytoprotective roles for TRAP1 in cellular stress responses including the unfolded protein response to ER stress [9-11] and autophagy [12, 13]. Together, these effects seem to contribute for TRAP1 protective effect against apoptosis [5, 14]. These anti-apoptotic functions contribute to human oncogenesis. TRAP1 expression is increased in numerous human malignancies [15-17]. Functionally, inhibition of mitochondrial TRAP1 and related chaperones killed numerous tumor cells but not normal cells [8]. Anti-apoptotic functions of TRAP1 confer tumor cells resistance against different chemotherapeutic agents [2, 15]. For these reasons, TRAP1 has been proposed as a potential biomarker and target for anticancer therapies. In this context, mitochondrial-targeted agents have been developed to selectively inhibit HSP90-like mitochondrial chaperones inducing cell death and reverting tumor cell multi-drug resistant phenotype [18].

It has been described that TRAP1 is overexpressed in a subset of lung adenocarcinomas [19, 20] and has been found to be more highly expressed in poor prognosis patients [21]. It was described that TRAP1 regulates proliferation, mitochondrial function, and has prognostic significance in non-small cell lung cancer (NSCLC) [21].

Despite the increased information regarding its cytoprotective functions, the characterization of TRAP1 antiapoptotic effects is far from being complete. The goal of this study is to better

1  
2  
3 define the role of TRAP1 in the A549 human NSCLC cell line, specifically the relationship  
4 between its mitochondrial function and role in cellular stress responses. To this end TRAP1  
5 expression was depleted in both A549 tumor and MRC-5 normal cell lines using siRNA and  
6  
7 TRAP1 deficient cells were evaluated to determine TRAP1-dependent processes that  
8  
9 contribute to cell viability.  
10  
11  
12  
13

## 14 MATERIALS AND METHODS

### 15 **Cell culture and siRNA transfection**

16  
17 Human A549 lung cancer cells and MRC-5 normal lung fibroblasts were purchased from  
18  
19 ATCC (LGC Standards, Middlesex, UK), and cultured in Iscove's Modified Dulbecco's  
20  
21 Medium (IMDM, 12440-046; Gibco, Paisley, UK) supplemented with 5% FBS (16000-044,  
22  
23 Gibco) and antibiotic/antimycotic solution (A5955, Sigma; St. Quentin Fallavier, France), at  
24  
25 37°C in humidified air with 5% CO<sub>2</sub>. Details on cell transfection protocols can be seen in the  
26  
27 supplementary information (SI).  
28  
29  
30  
31  
32

### 33 **Cell mass**

34  
35 Cell mass was measured by the Sulforhodamine B (SRB) assay [22]. Complete experimental  
36  
37 details can be seen in the SI.  
38  
39  
40

### 41 **Western blotting analysis**

42  
43 Details on Western blotting analyses can be found in detail in the supplementary material.  
44  
45  
46

### 47 **Real-time RT-PCR**

48  
49 The experimental procedure for RT-PCR can be found in detail in the SI.  
50  
51  
52

### 53 **Mitochondrial transmembrane electric potential ( $\Delta\psi_m$ ) and mitochondrial superoxide 54 anion**

55  
56  
57  
58  
59  
60

1  
2  
3 Mitochondrial transmembrane electric potential ( $\Delta\psi_m$ ) and mitochondrial superoxide anion  
4  
5 were evaluated using fluorescent dyes, as described in the SI.

### 6 7 **Mitochondrial permeability transition pore (mPTP) opening**

8  
9 Determination of mPTP opening was performed using the MitoProbe Transition Pore Assay  
10  
11 (M34153; Invitrogen) by co-loading with calcein-AM and  $\text{CoCl}_2$  as previously described  
12  
13 [23]. Further details are present in the supplementary materials and methods.

### 14 15 16 17 **Oxygen consumption and glycolytic fluxes**

18  
19 Oxygen consumption rates (OCR) and extracellular acidification rates (ECAR) were  
20  
21 measured using the Seahorse XF<sup>96</sup> Extracellular Flux Analyzer Technology (Seahorse  
22  
23 Biosciences; North Billerica, MA, USA), as described in detail in the SI.

### 24 25 26 27 **Adenine nucleotide measurement (ATP/ADP/AMP)**

28  
29 ATP, ADP and AMP levels were measured by HPLC as described in detail in the SI.

### 30 31 32 33 **Immunocytochemistry**

34  
35 The protocol for immunocytochemistry is detailed in the SI.

### 36 37 38 39 **Mitochondrial morphology and lysosome content**

40  
41 The experimental protocol for the evaluation of mitochondrial morphology and lysosomal  
42  
43 content is described in detail in the SI.

### 44 45 46 47 **Enzymatic activities**

48  
49 Activities of cysteine-proteinase cathepsin B, aspartate-proteinase cathepsin D, and caspases -  
50  
51 3, -7, and -9 were measured as described in detail in the SI.

### 52 53 54 55 **Live/dead assay**

1  
2  
3 Calcein-AM (C1430; Invitrogen) and Propidium Iodide (PI) (P4864; Sigma Aldrich) were  
4 used to determine the percentages of viable and dead cells. The detailed protocol can be found  
5 in the SI.  
6  
7  
8  
9

### 10 **Statistical analyses**

11 For statistical analysis of two means Student's t test was used while for comparisons of more  
12 than two groups an analysis of variances (ANOVA) with matched-pairs was used instead. In  
13 both cases, data was checked for normality using the Kolmogorov-Smirnov with Dallal-  
14 Wilkison-Lillie for correction and equality of variances using the F test or Bartlett's test in  
15 order to apply the statistical tests. Otherwise the respective non-parametric test was chosen:  
16 Mann-Whitney for t test and Friedman test for ANOVA.  
17  
18

19 In situations where one wanted to evaluate the effect of two variables a two-way ANOVA  
20 was applied following the same assumptions as mentioned earlier. Differences were  
21 considered significant at 5% level and p value was categorized accordingly to their interval of  
22 confidence. For one- and two-way ANOVA, corrections for multiple comparisons were made  
23 using Bonferroni post-hoc test using predefined comparisons, to decrease both type I and type  
24 II errors.  
25  
26  
27  
28  
29  
30  
31  
32  
33  
34  
35  
36  
37

## 38 **RESULTS**

### 39 **TRAP1 depletion caused decreased viability in A549 cells.**

40  
41  
42 We initially investigated by Western Blotting the amount of TRAP1 expressed in both A549  
43 and MRC-5 cell lines in order to identify differential expression levels. This experiment  
44 showed that A549 lung cancer cells showed the highest expression of TRAP1 (Fig. S1A)  
45  
46 To characterise the overall outcome of TRAP1 inhibition on mitochondrial physiology, a  
47 knockdown was performed in both A549 and MRC-5 cell lines using a siRNA construct  
48 (siTRAP1) (Fig. S1B).  
49  
50  
51  
52  
53

54 In accordance with previous reports [21, 24], TRAP1 silencing resulted in a decrease in tumor  
55 cell proliferation rate within 24 hours post-seeding leading to a 62% reduction of A549 cell  
56  
57  
58  
59  
60

1  
2  
3 mass during 72 hours (Fig. S1C). Increased cell death contributes to decreased viability as  
4 calcein-AM and propidium iodide Live/Death assay confirmed that A549 TRAP1 silencing  
5 increases the percentage of dead cells (Fig. S1D). Interestingly, TRAP1 silencing resulted in a  
6  
7 significant decrease in MRC-5 cell proliferation (Fig. S1C) leading to a drop of 49% in cell  
8  
9 mass.  
10  
11  
12  
13

### 14 **TRAP1 silencing resulted in mitochondrial dysfunction**

15  
16 As TRAP1 cytoprotective role has been mainly associated with its preferential mitochondrial  
17  
18 localization within tumor cells [25] we examined the effect of TRAP1 depletion on  
19  
20 mitochondrial function in A549 and MRC-5 cells. TRAP1 subcellular localization was  
21  
22 evaluated through cell imaging by co-staining cells with antibodies against TRAP1 and the  
23  
24 outer mitochondrial membrane marker TOM20. In agreement with the literature,  
25  
26 immunofluorescence assays showed TRAP1 co-localization with TOM20 in A549 control  
27  
28 cells (scrambled siRNA, siCTL) with a small amount of fluorescent signal dispersed  
29  
30 throughout the cell, as previously demonstrated [26] (Fig. 1A). Interestingly, even though  
31  
32 TRAP1 co-localization with TOM20 was also observed in MRC-5 cells, this mitochondrial  
33  
34 chaperone seems to have a sparse and diffused distribution in these cells, instead of the  
35  
36 expected major mitochondrial localization, suggesting TRAP1 preferentially localizes in  
37  
38 extra-mitochondrial sites in MRC-5 cells (Fig. S3A). No alteration in TOM20 protein content  
39  
40 was observed after TRAP1 silencing (Fig. S2A).  
41

42 Overall A549 siTRAP1 cells bioenergetic capacity was decreased as indicated by decreased  
43  
44 ATP/ADP ratio and adenylate energy charge (Fig. 1B), and decreased oxygen consumption,  
45  
46 both basal (Fig. 1C) and in the presence of the mitochondrial uncoupler FCCP (Fig. 1D)  
47  
48 although glycolytic rates remained unaltered upon TRAP1 silencing when indirectly inferred  
49  
50 through the evaluation of extracellular acidification rate (ECAR) (Fig. S2B). Further evidence  
51  
52 of disrupted electron transport chain was provided by increased Mitosox staining indicating  
53  
54 increased superoxide accumulation in TRAP1 depleted cells (Fig. 1E). Finally, mitochondrial  
55  
56 membrane potential was diminished as shown by decreased TMRM staining of TRAP1  
57  
58  
59  
60

1  
2  
3 depleted cells (Fig. 1F). Conversely, our findings indicate that TRAP1 silencing does not  
4  
5 lead to changes in MRC-5 oxidative stress levels and mitochondrial membrane potential (Fig.  
6  
7 S3B).

8  
9 Considering that mitochondrial depolarization together with decreased ATP production and  
10  
11 inhibition of respiration constitute some of the later stage effects of mPTP opening, and since  
12  
13 TRAP1 has been described to modulate mPTP by binding to and antagonizing CypD function  
14  
15 conferring tumor cells protection against apoptosis [8], the open/closed conformation of the  
16  
17 mPTP was measured. Surprisingly, TRAP1 depletion in A549 resulted in a more closed  
18  
19 mPTP conformation when compared to siCTL cells (Fig. 1G) suggesting other factors may be  
20  
21 contributing to the observed mitochondrial impairment, whereas in MRC-5 cells no changes  
22  
23 were observed in mPTP opening status (Fig. S3D). The results observed for the lung tumor  
24  
25 cell line were not due to defective CypD function in TRAP1 depleted cells as equivalent  
26  
27 CypD protein content was observed (Fig. S2C) and cyclosporin A was effective in closing the  
28  
29 mPTP (Fig. 1G). Thus, in these cells TRAP1 deficiency results in loss of mitochondrial  
30  
31 membrane potential through a means other than promoting opening of the mPTP.

### 32 33 34 **TRAP1 depletion altered mitochondrial morphology**

35  
36 Additionally, TRAP1 depletion in A549 cells was accompanied by alterations in  
37  
38 mitochondrial morphology while no changes in organelle morphology were observed between  
39  
40 the MRC-5 cell groups (Fig. S3E). Mitochondria were stained by Mitotracker Red (MTR) dye  
41  
42 to delineate morphology and morphology was quantitated. The average area/perimeter ratio  
43  
44 was employed as an index of mitochondrial interconnectivity and inverse circularity used to  
45  
46 ascertain mitochondrial elongation [27]. By these measures siTRAP1 A549 cells displayed  
47  
48 reduced elongation and interconnectivity, confirmed by staining with MTR (Fig. 2A). This  
49  
50 was accompanied by an increase in dynamin-related protein 1 (DRP1) levels with no  
51  
52 alterations of in expression of FIS1 or either of the mitochondrial fusion proteins, optic  
53  
54 atrophy protein 1 (OPA1) and mitofusin-1 (MFN1), suggesting that altered morphology

1  
2  
3 following TRAP1 silencing was due to enhanced mitochondrial fission (Fig. 2B). These  
4 observations, together with the fact that no alterations were found in the expression of the  
5 studied mitochondrial dynamics proteins in MRC-5 cells (Fig. S3F), highlight the role for  
6 TRAP1 in the maintenance of mitochondrial morphology, which would be more pertinent in  
7 cells under stress, such as in tumors.  
8  
9  
10  
11  
12

### 13 **TRAP1 silencing altered A549 cell death machinery**

14  
15 To determine how loss of mitochondrial membrane potential contributes to decreased cell  
16 viability and increased cell death, several apoptotic pathways were analyzed. Since A549  
17 cells do not express BCL-2 [28], the expression of pro-apoptotic BAX and anti-apoptotic  
18 BCL-xL proteins was measured to determine mitochondrial permeability mediated apoptosis  
19 was enhanced. TRAP1 silencing in these cells induced a significant increase in BAX protein  
20 content along with a marked decrease of BCL-xL (Fig. 3A) suggesting the activation of  
21 intrinsic apoptosis. The BAX/BCL-xL ratio was of  $2.10 \pm 0.18$  (n=6) for siTRAP1 cells and  
22  $0.79 \pm 0.03$  (n=6) for siCTL cells ( $p < 0.001$ ), with the difference mainly due to decreased BCL-  
23 xL expression. Therefore, TRAP1 seems to protect cells from mitochondrial apoptosis  
24 mainly through up-regulation of BCL-xL anti-apoptotic protein expression. Interestingly, the  
25 expression of BAX and BCL-2 proteins in MRC-5 cells showed a BAX/BCL-2 ratio of  
26  $1.06 \pm 0.07$  (n=4) for siTRAP1 and  $1.00 \pm 0.15$  (n=4) for siCTL group ( $p > 0.05$ ), indicating that  
27 in these normal cells, TRAP1 does not alter the pro- anti-apoptotic protein balance (Fig.  
28 S3G).  
29  
30  
31  
32  
33  
34  
35  
36  
37  
38  
39  
40  
41  
42

43 Notwithstanding, TRAP1 silencing increased expression of key proteases involved in cell  
44 death. siTRAP1 cells showed a higher expression of pro-caspase-3 (Fig. 3B) in A549 cells  
45 and increased activity of Caspase 3/7 in both A549 and MRC-5 cells (Fig. 3C and S3G).  
46  
47  
48

49 Cathepsins D and B are involved in processes of lysosomal cell death being able to activate  
50 caspases cascade and directly cleave pro-caspase-3 [29-31]. Increased cathepsin B activity  
51 was observed in A549 cells (Fig. 3D), despite reduced expression of cathepsins D and B and  
52 no change in cathepsin D activity (Fig. 3E).  
53  
54  
55  
56  
57  
58  
59  
60

1  
2  
3 To further delineate apoptosis pathways activated by TRAP1 silencing, we measured the  
4 activities of initiator caspases 8 and 9 (Fig. 3F) which are associated with extrinsic and  
5 intrinsic pathways, respectively. Our results argued against activation of classical apoptotic  
6 pathways after TRAP1 silencing since we did not find increases in initiator caspases 8  
7 (extrinsic) and 9 (intrinsic) activities in siTRAP1 A549 cells (Fig. 3F). However, it is  
8 important to note a higher caspase 9 activity was observed in siTRAP1 MRC-5 cells (Fig.  
9 S3G).

10  
11 Observations in the A549 cell line suggest the activation of alternative forms of cell death,  
12 possibly related with the development of acidic organelles and the activation of the lysosomal  
13 protease cathepsin B described above. Overall, our data suggests distinct forms of cell death  
14 pathways are activated as a result from TRAP1 depletion depending on the importance of this  
15 chaperone for mitochondrial maintenance in tumor vs normal lung cells.

#### 16 17 18 19 20 21 22 23 24 25 26 27 28 **Autophagy is altered in TRAP1 depleted cells.**

29  
30 Our results demonstrate mitochondrial damage with likely mitochondrial fission carried out  
31 by DRP1 in A549 TRAP1 depleted cells. As damaged mitochondria can be removed by  
32 autophagy we focused on the effect of TRAP1 on this process. Conversion of microtubule-  
33 associated protein 1A/1B-light chain 3 (LC3-I, 18-kDa) to LC3-II (16-kDa) is an essential  
34 step in the formation of the autophagic vesicle. Thus, accumulation of LC3-II is considered  
35 the most definitive marker for autophagosomes [32]. Initial measurements of basal LC3-II  
36 levels show no significant difference between TRAP1 expressing and TRAP1-depleted cells  
37 (Fig. 4A). However, since LC3-II is subjected to lysosomal degradation during autophagy,  
38 LC3-II levels do not accurately reflect autophagy induction. To test if autophagic flux is  
39 increased in TRAP1 depleted cells, LC3-II expression was analyzed in both siCTL and  
40 siTRAP1 A549 cells treated with Bafilomycin A1 (BafA1), a known inhibitor of the late  
41 phase of autophagy due to its effects in neutralizing acidic organelles [33]. Even though no  
42 differences were observed in non-treated siCTL and siTRAP1 cells, LC3-II content increased  
43 upon BafA1 treatment in both siCTL and siTRAP1 cells. However, LC3-II accumulation is  
44  
45  
46  
47  
48  
49  
50  
51  
52  
53  
54  
55  
56  
57  
58  
59  
60

1  
2  
3 significant and shows a greater fold change in siTRAP1 cells supporting increased autophagic  
4 flux after TRAP1 depletion (Fig. 4A). Although levels of several enzymes involved in  
5 autophagy are lower in TRAP1 depleted cells (Fig. 4B) further investigation provides  
6 evidence of increased autophagic flux. Disruption of autophagy often results in the  
7 accumulation of autophagy ubiquitin-binding adaptor p62/SQSTM1 (sequestosome-1) [34].  
8 In support of increased autophagic flux, p62 protein levels in siTRAP1 A549 cells were  
9 significantly decreased (Fig. 4B). Moreover, TRAP1 silencing in MRC-5 led to decreased  
10 ATG12-ATG5 complex, LC3 and p62 protein levels, also indicating an increase in autophagy  
11 flux in these cells (Fig. S4A).

12  
13 In addition, the area of lysotracker green labelled cellular organelles increased dramatically in  
14 siTRAP1 A549 cells, indicating an expansion of acidic organelles including the lysosome, the  
15 site of degradation of autophagic cargo (Fig. 4C). In addition, levels of LAMP2A protein, a  
16 lysosomal receptor involved in chaperone mediated autophagy (CMA) [35], are increased in  
17 TRAP1 depleted cells suggesting possible involvement of CMA (Fig. 4D). No differences  
18 were observed between siCTL and siTRAP1 MRC-5 cells for lysosomal content and CMA  
19 markers (Fig. S4A and B).

20  
21 To evaluate the effect of TRAP1 silencing on ER stress and the unfolded protein response  
22 (UPR) in A549 cells, we measured the expression of several key chaperones that have been  
23 implicated in TRAP1 mediated alteration of the UPR- HSP90, Glucose-regulated protein 78  
24 (GRP78) and GRP94. No alteration in the expression of these chaperones was detected,  
25 suggesting that TRAP1 silencing did not induce ER-stress and the consequent UPR in A549  
26 cells (Fig. S2D).

#### 27 28 29 30 31 32 33 34 35 36 37 38 39 40 41 42 43 44 45 46 47 48 49 50 51 52 53 54 **TRAP1 silencing altered the outcome of increased autophagy**

1  
2  
3 Autophagy plays a major role in maintaining cell quality control and homeostasis but under  
4  
5 extreme conditions autophagic signaling can be recruited to activate cell death pathways.  
6  
7 Thus, autophagy can act either as a tumor suppressor or as a tumor maintenance factor [36,  
8  
9 37]. To better understand the functional significance of the autophagic activation observed in  
10  
11 siTRAP1 cells, transfected cells were treated with either the autophagy inducer rapamycin or  
12  
13 the autophagy inhibitor 3-methyladenine (3-MA) for up to 72 hours and evaluated for cell  
14  
15 viability. Inhibition of autophagy by inhibition of lysosomal acidification with 3-MA leads to  
16  
17 decreased cell viability in both TRAP1-expressing and TRAP1-depleted A549 cells indicating  
18  
19 that autophagy promotes cell viability in these cells (Fig. 5A). Although similar observations  
20  
21 were made for MRC-5 cells, the decrease in siCTL cell mass upon treatment with 3-MA is  
22  
23 not as strong, leading to an overall decrease of only about 20% whereas this difference  
24  
25 reaches a value of 400% for the correspondent A549 cell groups (siCTL vs siCTL treated  
26  
27 with 3-MA) (Fig. 5A and Fig. S4C). In contrast, treatment with Rapamycin, which activates  
28  
29 autophagy by inhibition of mammalian target of rapamycin (mTOR), showed contradictory  
30  
31 results. As expected, activation of autophagy is protective for A549 TRAP1 depleted cells.  
32  
33 However, Rapamycin treatment of TRAP1 expressing cells is severely deleterious to these  
34  
35 cells in contrast with what is observed for MRC-5 cells (Fig. 5B). Induction of autophagy in  
36  
37 MRC-5 cells resulted in a significant cell mass decrease in siCTL cells with no change  
38  
39 observed for the TRAP1-depleted cells (Fig. S4C).

40  
41 These results demonstrate that autophagy at endogenous levels is protective for TRAP1  
42  
43 expressing A549 cells. However, the effect of activation of autophagy above endogenous  
44  
45 levels is context dependent and TRAP1 expression levels alter this context. Mechanistically,  
46  
47 both increased endogenous autophagic flux and increased tolerance for induced autophagy in  
48  
49 A549 TRAP1-depleted cells may be a consequence of mitochondrial dysfunction creating a  
50  
51 greater need for autophagic mitophagy to remove damaged mitochondria which our results  
52  
53 suggest might be specific to tumor cells.  
54  
55  
56  
57  
58  
59  
60

## DISCUSSION

In agreement with previous studies [25], we found that TRAP1 co-localizes with mitochondria in A549 cells, based on co-localization with the outer-mitochondrial protein TOM20. In addition, TRAP1-depleted cells showed impairment of multiple parameters of mitochondrial function as previously reported including decreased  $\Delta\Psi_m$ , increased ROS production, and lower oxygen consumption. The increased mitochondrial ROS production in TRAP1-depleted cells can trigger cell death by mPTP opening, which in turn results in  $\Delta\Psi_m$  loss. TRAP1, along with HSP90 mitochondrial pool and HSP60, have been described to physically interact with matrix CypD modulating its regulatory activity and resulting in mPTP inhibition [3, 8]. Surprisingly, TRAP1-depletion resulted in a more closed mPTP conformation under basal conditions, which was the opposite effect to that observed in melanoma [38]. Our result was not due to loss of CypD expression or activity as CypD expression was intact and addition of cyclosporin-A resulted in an increase in mPTP closing. The discrepancy with previous work may reflect that these studies relied on extrapolation of mPTP status from analysis of  $\Delta\Psi_m$  alterations [8] or on evaluation of cell viability in the presence or absence of CsA [3]. These results suggest that TRAP1 can influence mitochondrial-mediated viability in A549 cells by means other than inhibition of CypD. Accumulation of depolarized mitochondria and oxidative damage has been associated with the occurrence of mitochondrial fusion and fission processes in an attempt to either restore homeostasis or eliminate mitochondria that are beyond repair [39]. Consistent with mitochondrial impairment, TRAP1 depletion has been reported to result in altered mitochondrial morphology, including both fragmentation [40] and formation of tubules [41]. Here, TRAP1 silencing in tumor cell line resulted altered mitochondrial morphology characterized by the accumulation of smaller and rounder mitochondria and increased expression of the fission protein DRP1 without affecting expression of FIS1 or the fusion proteins MFN1 and OPA1.

Our results suggests that TRAP1 may differentially localize in normal (MRC-5) versus tumor (A549) cells which might explain why TRAP1 depletion in MRC-5 cells had no implications

1  
2  
3 on mitochondrial physiology and morphology. Based on our observations, we hypothesized  
4 that TRAP1 preferentially localize to extramitochondrial sites in normal cells thus not having  
5 such an important role in mitochondrial homeostasis maintenance.  
6  
7

8  
9 The process of mitochondrial fragmentation has been reported to occur almost simultaneously  
10 with pro- apoptotic BCL-2 family member BAX translocation to mitochondria but before  
11 caspases activation [42]. In addition to increased mitochondrial fragmentation, A549 TRAP1-  
12 depleted cells showed elevated BAX and reduced BCL-xL protein levels. This shift in the  
13 balance between pro-apoptotic and pro-survival BCL-2 family proteins was accompanied by  
14 an increase in the expression and activity of caspase 3. Surprisingly, caspase 3/7 activation in  
15 A549 TRAP1-depleted cells appears to occur in a caspase 8 and/or 9-independent manner  
16 suggesting that in these cells, caspase 3/7 undergo activation through alternative pathways.  
17 Increased activity of cathepsin B suggests that some degree of lysosomal permeabilization  
18 may be occurring. Cytosolic cathepsins may contribute to degradation of BCL-xL [43] and  
19 activation of caspase 3 [44]. These results argue that decreased cell viability and increased  
20 cell death in A549 TRAP1-depleted cells are due to an apoptotic process.  
21  
22

23  
24 TRAP1 depletion is associated with activation of cellular stress responses including ER stress  
25 protection [11] and mitochondrial UPR in *Drosophila* [45] and activation of autophagy and  
26 the UPR in tumor cells [9]. Since these responses can activate apoptotic pathways we  
27 investigated their role in TRAP1-depleted loss of cell viability. Our studies showed loss of  
28  $\Delta\Psi_m$ , mitochondrial fragmentation and increased expression of DRP1 all of which are  
29 associated with accumulation of damaged mitochondria and activation of macroautophagy to  
30 remove them [46, 47]. A549 siTRAP cells showed a marked increase in the overall lysosome  
31 content suggesting activation of autophagy which transports cargo to the lysosome for  
32 degradation.  
33  
34

35  
36 Initial studies showed that TRAP1 silencing resulted in a generalized decrease in the  
37 expression of enzymes involved in the autophagic pathway, such as BECLIN-1, and proteins  
38 that are part of both ATG12 and LC3 ubiquitin-like systems. However, enzyme levels do not  
39 reflect autophagic flux [32]. Measurement of autophagic substrate SQSTM1 levels showed  
40  
41  
42  
43  
44  
45  
46  
47  
48  
49  
50  
51  
52  
53  
54  
55  
56  
57  
58  
59  
60

1  
2  
3 decreased expression in TRAP1 depleted cells. Further, the accumulation of LC3-II upon  
4 inhibition of late phase autophagy with Bafilomycin A supports an increase in the autophagic  
5 flux in cells with decreased TRAP1 expression. In addition, increased levels of the lysosomal  
6 receptor for chaperone-mediated autophagy (CMA) cargo, LAMP2A, raise the possibility that  
7 CMA is also involved. No change in expression of the UPR-related chaperones HSP90,  
8 GRP78 and GRP94 was measured suggesting that TRAP1 depletion in these cells may not  
9 alter the UPR.  
10

11  
12 As disturbances in the autophagy flux has been associated with cancer development and  
13 progression [48], our results suggest that autophagy in A549 cells constitutes a mechanism to  
14 promote cell survival. Additionally, the effect of rapamycin treatment in TRAP1-silenced  
15 cells growth reinforces the role of this chaperone in the regulation of survival autophagy.  
16 Inhibition of autophagy by treatment with 3-MA leads to decreased cell viability in both  
17 TRAP1-expressing and TRAP-depleted cells indicating that autophagy promotes cell viability  
18 in these cells. However, treatment with Rapamycin, predicted to activate autophagy by  
19 inhibition of mTOR, showed contradictory results. Interestingly, TRAP1-depleted cells  
20 proliferation after rapamycin treatment was higher than their basal growth and control cells  
21 incubated with the same drug showed similar proliferation rates to that of non-treated  
22 siTRAP1 cells. The later observations show that by stimulating autophagy in TRAP1-  
23 expressing tumor cells it may be possible to mimic the effect of TRAP1 inhibition. These  
24 results demonstrate that autophagy at endogenous levels is protective for A549 cells. **In**  
25 **contrast, autophagy inhibition does not seem to have a strong effect on MRC-5 cells whereas**  
26 **autophagy induction leads to a higher decrease in overall cell viability.**  
27

28  
29 Altogether these results highlight TRAP1 involvement in the main cellular quality control  
30 mechanisms concerning the lysosomal system in the A549 tumor cell line. Autophagy  
31 activation upon TRAP1 silencing in these cells seems to have a protective role in maintaining  
32 homeostasis upon loss of the mitochondrial chaperone. However, TRAP1 depletion results in  
33 mitochondrial damage in tumor cells, consequent accumulation of misfolded proteins and  
34  
35  
36  
37  
38  
39  
40  
41  
42  
43  
44  
45  
46  
47  
48  
49  
50  
51  
52  
53  
54  
55  
56  
57  
58  
59  
60

1  
2  
3 damaged organelles, to which cells respond by increasing autophagy levels to avoid  
4  
5 apoptosis.

6  
7 The translation of our *in vitro* data to clinical application is not straightforward. One current  
8  
9 limitation is the lack of *in vivo* evidence that TRAP1 targeting by pharmacological means  
10  
11 inhibits tumour growth. In fact, the effectiveness of targeted therapies for cancers is  
12  
13 extremely context dependent. For example, the complexity of the role of autophagy in  
14  
15 therapeutic responses to therapy in NSCLC has been demonstrated [49]. Furthermore, recent  
16  
17 data demonstrated that cytosolic Hsp90alpha and TRAP1 modulate growth and lung  
18  
19 metastasis *in vivo*, although they do not play any role in the initiation of breast cancer. It  
20  
21 remains to be demonstrated whether the same occurs in lung cancer and whether modulation  
22  
23 of autophagy plays a role [50].

24 **In conclusion, our study provides evidence that modulation of TRAP1 expression influences**  
25 **the effect of autophagy on A549 cell viability providing new insights to possible therapeutic**  
26 **approaches regarding TRAP1 overexpressing tumors as the described results support the**  
27 **hypothesis that autophagy inhibition could constitute a good approach to induce tumor cell**  
28 **death with no strong implications to normal cells.**  
29  
30  
31  
32  
33

#### 34 35 36 37 38 ACKNOWLEDGEMENTS

39  
40 Sponsored by the European Regional Development Fund (ERDF) through the COMPETE  
41  
42 2020 - Operational Programme for Competitiveness and Internationalisation and Portuguese  
43  
44 national funds via FCT–Fundação para a Ciência e a Tecnologia, projects POCI-01-0145-  
45  
46 FEDER-016390: CANCEL STEM, and IF/01316/2014. Also supported by POCI-01-0145-  
47  
48 FEDER-007440, and PCTI project (Government of the Principality of Asturias and ERDF)  
49  
50 with reference GRUPIN14-071. The funding agencies had no role in study design,  
51  
52 experimentation, or writing the manuscript. The authors have no conflict of interests.  
53  
54  
55  
56  
57  
58  
59  
60

1  
2  
3  
4  
5  
6  
7  
8  
9  
10  
11  
12  
13  
14  
15  
16  
17  
18  
19  
20  
21  
22  
23  
24  
25  
26  
27  
28  
29  
30  
31  
32  
33  
34  
35  
36  
37  
38  
39  
40  
41  
42  
43  
44  
45  
46  
47  
48  
49  
50  
51  
52  
53  
54  
55  
56  
57  
58  
59  
60

AUTHOR CONTRIBUTIONS

IAB, IVN, RL, AFB, RG performed the research work; IAB, IVN, PMS, PJO wrote the manuscript; IAB prepared the figures; PJO, IVN and PMS provided supervision of the work; all authors critically read the manuscript and approved its submission.

For Review Only

## REFERENCES

- 1 Koh H and Chung J. PINK1 as a molecular checkpoint in the maintenance of mitochondrial function and integrity. *Mol Cells* 2012;**34**:7-13.
- 2 Landriscina M, Laudiero G, Maddalena F, Amoroso MR, Piscazzi A, Cozzolino F *et al.* Mitochondrial chaperone Trap1 and the calcium binding protein Sorcin interact and protect cells against apoptosis induced by antiproliferative agents. *Cancer Res* 2010;**70**:6577-86.
- 3 Xiang F, Huang YS, Shi XH and Zhang Q. Mitochondrial chaperone tumour necrosis factor receptor-associated protein 1 protects cardiomyocytes from hypoxic injury by regulating mitochondrial permeability transition pore opening. *FEBS J* 2010;**277**:1929-38.
- 4 Zhang Y, Jiang DS, Yan L, Cheng KJ, Bian ZY and Lin GS. HSP75 protects against cardiac hypertrophy and fibrosis. *J Cell Biochem* 2011;**112**:1787-94.
- 5 Montesano Gesualdi N, Chirico G, Pirozzi G, Costantino E, Landriscina M and Esposito F. Tumor necrosis factor-associated protein 1 (TRAP-1) protects cells from oxidative stress and apoptosis. *Stress* 2007;**10**:342-50.
- 6 Hua G, Zhang Q and Fan Z. Heat shock protein 75 (TRAP1) antagonizes reactive oxygen species generation and protects cells from granzyme M-mediated apoptosis. *J Biol Chem* 2007;**282**:20553-60.
- 7 Im CN, Lee JS, Zheng Y and Seo JS. Iron chelation study in a normal human hepatocyte cell line suggests that tumor necrosis factor receptor-associated protein 1 (TRAP1) regulates production of reactive oxygen species. *J Cell Biochem* 2007;**100**:474-86.

- 1  
2  
3 8 Kang BH, Plescia J, Dohi T, Rosa J, Doxsey SJ and Altieri DC. Regulation of  
4 tumor cell mitochondrial homeostasis by an organelle-specific Hsp90  
5 chaperone network. *Cell* 2007;**131**:257-70.  
6  
7  
8  
9 9 Amoroso MR, Matassa DS, Laudiero G, Egorova AV, Polishchuk RS,  
10 Maddalena F *et al.* TRAP1 and the proteasome regulatory particle TBP7/Rpt3  
11 interact in the endoplasmic reticulum and control cellular ubiquitination of  
12 specific mitochondrial proteins. *Cell Death Differ* 2012;**19**:592-604.  
13  
14  
15  
16  
17 10 Siegelin MD, Dohi T, Raskett CM, Orlowski GM, Powers CM, Gilbert CA *et*  
18 *al.* Exploiting the mitochondrial unfolded protein response for cancer therapy  
19 in mice and human cells. *J Clin Invest* 2011;**121**:1349-60.  
20  
21  
22  
23  
24 11 Takemoto K, Miyata S, Takamura H, Katayama T and Tohyama M.  
25 Mitochondrial TRAP1 regulates the unfolded protein response in the  
26 endoplasmic reticulum. *Neurochem Int* 2011;**58**:880-7.  
27  
28  
29  
30  
31 12 Caino MC, Chae YC, Vaira V, Ferrero S, Nosotti M, Martin NM *et al.*  
32 Metabolic stress regulates cytoskeletal dynamics and metastasis of cancer  
33 cells. *J Clin Invest* 2013;**123**:2907-20.  
34  
35  
36  
37 13 Chae YC, Caino MC, Lisanti S, Ghosh JC, Dohi T, Danial NN *et al.* Control  
38 of tumor bioenergetics and survival stress signaling by mitochondrial HSP90s.  
39 *Cancer Cell* 2012;**22**:331-44.  
40  
41  
42  
43 14 Masuda Y, Shima G, Aiuchi T, Horie M, Hori K, Nakajo S *et al.* Involvement  
44 of tumor necrosis factor receptor-associated protein 1 (TRAP1) in apoptosis  
45 induced by beta-hydroxyisovalerylshikonin. *J Biol Chem* 2004;**279**:42503-15.  
46  
47  
48  
49 15 Costantino E, Maddalena F, Calise S, Piscazzi A, Tirino V, Fersini A *et al.*  
50 TRAP1, a novel mitochondrial chaperone responsible for multi-drug  
51  
52  
53  
54  
55  
56  
57  
58  
59  
60

- 1  
2  
3 resistance and protection from apoptosis in human colorectal carcinoma cells.  
4  
5 *Cancer Lett* 2009;**279**:39-46.  
6
- 7 16 Fang W, Li X, Jiang Q, Liu Z, Yang H, Wang S *et al.* Transcriptional patterns,  
8  
9 biomarkers and pathways characterizing nasopharyngeal carcinoma of  
10  
11 Southern China. *J Transl Med* 2008;**6**:32.  
12
- 13 17 Leav I, Plescia J, Goel HL, Li J, Jiang Z, Cohen RJ *et al.* Cytoprotective  
14  
15 mitochondrial chaperone TRAP-1 as a novel molecular target in localized and  
16  
17 metastatic prostate cancer. *Am J Pathol* 2010;**176**:393-401.  
18
- 19 18 Siegelin MD. Inhibition of the mitochondrial Hsp90 chaperone network: a  
20  
21 novel, efficient treatment strategy for cancer? *Cancer Lett* 2013;**333**:133-46.  
22  
23
- 24 19 Cerami E, Gao J, Dogrusoz U, Gross BE, Sumer SO, Aksoy BA *et al.* The  
25  
26 cBio cancer genomics portal: an open platform for exploring multidimensional  
27  
28 cancer genomics data. *Cancer Discov* 2012;**2**:401-4.  
29
- 30 20 Gao J, Aksoy BA, Dogrusoz U, Dresdner G, Gross B, Sumer SO *et al.*  
31  
32 Integrative analysis of complex cancer genomics and clinical profiles using  
33  
34 the cBioPortal. *Sci Signal* 2013;**6**:p11.  
35  
36
- 37 21 Agorreta J, Hu J, Liu D, Delia D, Turley H, Ferguson DJ *et al.* TRAP1  
38  
39 regulates proliferation, mitochondrial function, and has prognostic  
40  
41 significance in NSCLC. *Mol Cancer Res* 2014;**12**:660-9.  
42  
43
- 44 22 Skehan P, Storeng R, Scudiero D, Monks A, McMahon J, Vistica D *et al.* New  
45  
46 colorimetric cytotoxicity assay for anticancer-drug screening. *J Natl Cancer*  
47  
48 *Inst* 1990;**82**:1107-12.  
49
- 50 23 Petronilli V, Miotto G, Canton M, Brini M, Colonna R, Bernardi P *et al.*  
51  
52 Transient and long-lasting openings of the mitochondrial permeability  
53  
54  
55  
56  
57  
58  
59  
60

- 1  
2  
3 transition pore can be monitored directly in intact cells by changes in  
4  
5 mitochondrial calcein fluorescence. *Biophys J* 1999;**76**:725-34.  
6
- 7 24 Tian X, Ma P, Sui CG, Meng FD, Li Y, Fu LY *et al.* Suppression of tumor  
8  
9 necrosis factor receptor-associated protein 1 expression induces inhibition of  
10  
11 cell proliferation and tumor growth in human esophageal cancer cells. *FEBS J*  
12  
13 2014;**281**:2805-19.  
14
- 15 25 Felts SJ, Owen BA, Nguyen P, Trepel J, Donner DB and Toft DO. The hsp90-  
16  
17 related protein TRAP1 is a mitochondrial protein with distinct functional  
18  
19 properties. *J Biol Chem* 2000;**275**:3305-12.  
20
- 21 26 Cechetto JD and Gupta RS. Immunoelectron microscopy provides evidence  
22  
23 that tumor necrosis factor receptor-associated protein 1 (TRAP-1) is a  
24  
25 mitochondrial protein which also localizes at specific extramitochondrial sites.  
26  
27 *Exp Cell Res* 2000;**260**:30-9.  
28
- 29 27 Dagda RK, Cherra SJ, 3rd, Kulich SM, Tandon A, Park D and Chu CT. Loss  
30  
31 of PINK1 function promotes mitophagy through effects on oxidative stress  
32  
33 and mitochondrial fission. *J Biol Chem* 2009;**284**:13843-55.  
34  
35
- 36 28 Bojes HK, Suresh PK, Mills EM, Spitz DR, Sim JE and Kehrer JP. Bcl-2 and  
37  
38 Bcl-xL in peroxide-resistant A549 and U87MG cells. *Toxicol Sci*  
39  
40 1998;**42**:109-16.  
41  
42
- 43 29 Ben-Ari Z, Mor E, Azarov D, Sulkes J, Tor R, Cheporko Y *et al.* Cathepsin B  
44  
45 inactivation attenuates the apoptotic injury induced by ischemia/reperfusion of  
46  
47 mouse liver. *Apoptosis* 2005;**10**:1261-9.  
48  
49
- 50 30 Johansson AC, Steen H, Ollinger K and Roberg K. Cathepsin D mediates  
51  
52 cytochrome c release and caspase activation in human fibroblast apoptosis  
53  
54 induced by staurosporine. *Cell Death Differ* 2003;**10**:1253-9.  
55  
56  
57  
58  
59  
60

- 1  
2  
3 31 Zheng X, Chu F, Mirkin BL, Sudha T, Mousa SA and Rebbaa A. Role of the  
4 proteolytic hierarchy between cathepsin L, cathepsin D and caspase-3 in  
5 regulation of cellular susceptibility to apoptosis and autophagy. *Biochim*  
6 *Biophys Acta* 2008;**1783**:2294-300.  
7  
8  
9  
10  
11 32 Klionsky DJ, Abdelmohsen K, Abe A, Abedin MJ, Abeliovich H, Acevedo  
12 Arozena A *et al.* Guidelines for the use and interpretation of assays for  
13 monitoring autophagy (3rd edition). *Autophagy* 2016;**12**:1-222.  
14  
15  
16  
17  
18 33 Yang YP, Hu LF, Zheng HF, Mao CJ, Hu WD, Xiong KP *et al.* Application  
19 and interpretation of current autophagy inhibitors and activators. *Acta*  
20 *Pharmacol Sin* 2013;**34**:625-35.  
21  
22  
23  
24 34 Bjorkoy G, Lamark T, Pankiv S, Overvatn A, Brech A and Johansen T.  
25 Monitoring autophagic degradation of p62/SQSTM1. *Methods Enzymol*  
26 2009;**452**:181-97.  
27  
28  
29  
30  
31 35 Kaushik S and Cuervo AM. Chaperone-mediated autophagy: a unique way to  
32 enter the lysosome world. *Trends Cell Biol* 2012;**22**:407-17.  
33  
34  
35 36 Gozuacik D and Kimchi A. Autophagy as a cell death and tumor suppressor  
36 mechanism. *Oncogene* 2004;**23**:2891-906.  
37  
38  
39 37 Ogier-Denis E and Codogno P. Autophagy: a barrier or an adaptive response  
40 to cancer. *Biochim Biophys Acta* 2003;**1603**:113-28.  
41  
42  
43  
44 38 Basit F, van Oppen LM, Schockel L, Bossenbroek HM, van Emst-de Vries  
45 SE, Hermeling JC *et al.* Mitochondrial complex I inhibition triggers a  
46 mitophagy-dependent ROS increase leading to necroptosis and ferroptosis in  
47 melanoma cells. *Cell Death Dis* 2017;**8**:e2716.  
48  
49  
50  
51  
52 39 Youle RJ and van der Bliek AM. Mitochondrial fission, fusion, and stress.  
53 *Science* 2012;**337**:1062-5.  
54  
55  
56  
57  
58  
59  
60

- 1  
2  
3 40 Butler EK, Voigt A, Lutz AK, Toegel JP, Gerhardt E, Karsten P *et al.* The  
4 mitochondrial chaperone protein TRAP1 mitigates alpha-Synuclein toxicity.  
5  
6  
7 *PLoS Genet* 2012;**8**:e1002488.  
8
- 9 41 Takamura H, Koyama Y, Matsuzaki S, Yamada K, Hattori T, Miyata S *et al.*  
10 TRAP1 controls mitochondrial fusion/fission balance through Drp1 and Mff  
11 expression. *PLoS One* 2012;**7**:e51912.  
12  
13  
14  
15 42 Youle RJ and Karbowski M. Mitochondrial fission in apoptosis. *Nat Rev Mol*  
16 *Cell Biol* 2005;**6**:657-63.  
17  
18  
19 43 de Castro MAG, Bunt G and Wouters FS. Cathepsin B launches an apoptotic  
20 exit effort upon cell death-associated disruption of lysosomes. *Cell Death*  
21 *Discovery* 2016;**2**:16012.  
22  
23  
24  
25 44 Johansson AC, Appelqvist H, Nilsson C, Kagedal K, Roberg K and Ollinger  
26 K. Regulation of apoptosis-associated lysosomal membrane permeabilization.  
27  
28 *Apoptosis* 2010;**15**:527-40.  
29  
30  
31  
32 45 Morrow G, Kim HJ, Pellerito O, Bourrelle-Langlois M, Le Pecheur M,  
33 Groebe K *et al.* Changes in Drosophila mitochondrial proteins following  
34 chaperone-mediated lifespan extension confirm a role of Hsp22 in  
35 mitochondrial UPR and reveal a mitochondrial localization for cathepsin D.  
36  
37  
38  
39  
40  
41  
42 *Mech Ageing Dev* 2016;**155**:36-47.  
43
- 44 46 Twig G, Elorza A, Molina AJ, Mohamed H, Wikstrom JD, Walzer G *et al.*  
45 Fission and selective fusion govern mitochondrial segregation and elimination  
46 by autophagy. *EMBO J* 2008;**27**:433-46.  
47  
48  
49
- 50 47 Rodriguez-Enriquez S, He L and Lemasters JJ. Role of mitochondrial  
51 permeability transition pores in mitochondrial autophagy. *Int J Biochem Cell*  
52 *Biol* 2004;**36**:2463-72.  
53  
54  
55  
56  
57  
58  
59  
60

- 1  
2  
3 48 Levine B and Kroemer G. Autophagy in the pathogenesis of disease. *Cell*  
4 2008;**132**:27-42.  
5  
6  
7 49 Saleh T, Cuttino L and Gewirtz DA. Autophagy is not uniformly  
8 cytoprotective: a personalized medicine approach for autophagy inhibition as a  
9 therapeutic strategy in non-small cell lung cancer. *Biochim Biophys Acta*  
10 2016.  
11  
12  
13  
14  
15 50 Vartholomaiou E, Madon-Simon M, Hagmann S, Muhlebach G, Wurst W,  
16 Floss T *et al.* Cytosolic Hsp90alpha and its mitochondrial isoform Trap1 are  
17 differentially required in a breast cancer model. *Oncotarget* 2017;**8**:17428-42.  
18  
19  
20  
21  
22  
23  
24  
25  
26  
27  
28  
29  
30  
31  
32  
33  
34  
35  
36  
37  
38  
39  
40  
41  
42  
43  
44  
45  
46  
47  
48  
49  
50  
51  
52  
53  
54  
55  
56  
57  
58  
59  
60

## FIGURE LEGENDS

Figure 1. TRAP1 silencing results in mitochondrial dysfunction. **(A)** Confocal images illustrate siTRAP1 and siCTL cells labeled with anti-TOM20 and anti-TRAP1 antibodies to determine TOM20 and TRAP1 co-localization. DAPI labels nuclei. Scale bar = 8  $\mu$ m. **(B)** ATP, ADP and AMP measurements taken by HPLC indicate a decreased ATP/ADP ratio and energy charge in siTRAP1 cells. **(C)** Basal oxygen consumption measured with a Seahorse XF<sup>96</sup> Extracellular Flux Analyzer and displayed as oxygen consumption rate (OCR) is higher in siCTL than in siTRAP1 cells. Data are means  $\pm$  SEM from n = 3 experiments. **(D)** Measurement of oxygen consumption rate (OCR) in both types of A549 cells using Seahorse Biosciences assay plates shows decreased respiration in siTRAP1 cells. Graphs are representative of three independent experiments and show the effects of mitochondrial inhibitors, (a) Oligomycin (2.5  $\mu$ M), (b) and (c) FCCP (500 nM) and (d) antimycin A (2.5  $\mu$ M) plus rotenone (2.5  $\mu$ M) injected as indicated. **(E)** Images of MitoSOX fluorescence in siTRAP1 and siCTL cells show an increase in mitochondrial superoxide anion production in siTRAP1 cells. Scale bar = 8  $\mu$ m. **(F)** TMRM fluorescence measured by flow cytometry reveals a lower mitochondrial membrane potential in siTRAP1 cells. Data are shown as relative fluorescence units (RFU) that represent the mean average of geometric mean values  $\pm$  SEM from three independent experiments. **(G)** Flow cytometric measurement of cobalt quenching of calcein fluorescence as an end-point for mPTP opening reveal a more closed conformation in siTRAP1 than in siCTL cells. Cyclosporin A (2  $\mu$ M) was able to close the pore in both types of A549 cells. Data are shown as relative fluorescence units (RFU) that represent the mean average of geometric mean values  $\pm$  SEM, normalized to fluorescence of cells incubated with calcein only for n=3. \*p<0.05; \*\* p<0.01; \*\*\* p<0.001 vs. siCTL cells.

Figure 2. TRAP1 silencing results in mitochondrial fragmentation. **(A)** Confocal images obtained using MitoTracker Red (MTR) for mitochondrial labeling and DAPI for nuclear labeling show alterations in mitochondrial morphology between siCTL and siTRAP1 A549

1  
2  
3 cells. Bar charts shows mitochondrial elongation and interconnectivity measured using Image  
4 J in fluorescent images of siCTL and siTRAP1 cells stained with MTR. Data show mean  $\pm$   
5 SEM from three separate experiments (15 cells per experimental condition and experiment).  
6  
7  
8 **(B)** Levels of proteins involved in mitochondrial dynamics (DRP1, FIS1, MFN1 and OPA1)  
9 indicate the occurrence of mitochondrial fission in siTRAP1 cells. Bar charts show means of  
10 optical density (O.D.)  $\pm$  SEM normalized to actin, from at least three separate immunoblots.  
11  
12  
13  
14 \* $p < 0.05$ ; \*\*\*  $p < 0.001$  vs. siCTL cells.  
15  
16  
17

18  
19 Figure 3. TRAP1 silencing alters cell death machinery. Expression of proteins involved in  
20 cell death **(A)** BAX, BCL-xL, and **(B)** caspase-3 indicates alterations in apoptotic  
21 pathways in A549 cells transfected with a TRAP1 siRNA (siTRAP1) in comparison with  
22 A549 cells transfected with a scrambled siRNA (siCTL). Bar charts show means of optical  
23 density (O.D.)  $\pm$  SEM normalized to actin, from at least three separate immunoblots. **(C)**  
24 Caspase 3/7-like activity showed an over-activation of caspase 3/7-like activity in siTRAP1  
25 cells. **(D)** Cathepsin D and B activities were determined to test the activation of lysosomal  
26 processes of cell death, showing cathepsin B activation in siTRAP1 cells. Data are means of  
27 enzymatic units per mg of protein  $\pm$  SEM, from at least five independent experiments. **(E)**  
28 Immunoblot analysis against cathepsin D and cathepsin B shows decreased expression of both  
29 proteases upon TRAP1 silencing. **(F)** Caspases 8-, 9-like activities determined in both types  
30 of A549 cells showed no alterations in the initiator caspases. **(G)** Representative western  
31 blots. Data are expressed as means  $\pm$  SEM from at least three independent experiments. Bar  
32 charts show means of optical density (O.D.)  $\pm$  SEM normalized to actin, from at least three  
33 separate immunoblots. \*  $p < 0.05$ ; \*\*  $p < 0.01$ ; \*\*\*  $p < 0.001$  vs. siCTL cells.  
34  
35  
36  
37  
38  
39  
40  
41  
42  
43  
44  
45  
46  
47  
48  
49

50  
51 Figure 4. TRAP1 silencing activates macroautophagy. **(A)** LC3 protein expression analysis  
52 reveals no alterations in the amount of the marker of autophagosomes LC3-II between both  
53 types of A549 cells. To evaluate autophagic flux, both types of cells were treated with  
54  
55  
56  
57  
58  
59  
60

1  
2  
3 bafilomycin A (BafA1) showing a higher accumulation of LC3-II in siTRAP1 cells. Bar  
4 charts show means of optical density (O.D.)  $\pm$  SEM normalized to actin, from at least three  
5 separate immunoblots. **(B)** Immunoblot analysis against the autophagy-related proteins  
6 BECLIN-1, ATG5, ATG12, ATG3 and ATG7 suggests a down-regulation in the autophagic  
7 machinery in A549 cells transfected with a TRAP1 siRNA (siTRAP1) in comparison with  
8 A549 cells transfected with a scrambled siRNA (siCTL). However, p62 expression was  
9 lower in siTRAP1 cells indicating that autophagic flux is higher in TRAP1-silenced cells. **(C)**  
10 Labelling of acidic compartments using LysoTracker Green reveals the development of acidic  
11 organelles after TRAP1 silencing. Histogram shows means of corrected total cell fluorescence  
12  $\pm$  SEM from three independent experiments (15 cells per experimental condition and  
13 experiment). **(D)** Protein expression of HCS70 shows no changes after TRAP1 depletion but  
14 LAMP-2A receptor shows a higher protein expression in siTRAP1 cells. Bar charts show  
15 means of optical density (O.D.)  $\pm$  SEM normalized to actin, from at least three separate  
16 immunoblots. \*  $p < 0.05$ ; \*\*  $p < 0.01$ ; \*\*\*  $p < 0.001$  vs. siCTL cells.  
17  
18  
19  
20  
21  
22  
23  
24  
25  
26  
27  
28  
29  
30  
31

32 Figure 5. Effect of the autophagic drugs, **(A)** 3-methyladenine (3-MA, 5 mM), and **(B)**  
33 rapamycin (100 nM), on cell viability. Rapamycin increased the proliferation of siTRAP1.  
34 Data are expressed as percentage of the control (vehicle only) for each time point. Data are  
35 means  $\pm$  SEM from  $n=5$ . # Represents comparison with siTRAP1 cells treated with either  
36 rapamycin or 3-MA, \* represents comparison with siTRAP1 cells, and • represents  
37 comparison with siCTL cells treated either with rapamycin or 3-MA.  
38  
39  
40  
41  
42  
43  
44  
45  
46  
47  
48  
49  
50  
51  
52  
53  
54  
55  
56  
57  
58  
59  
60

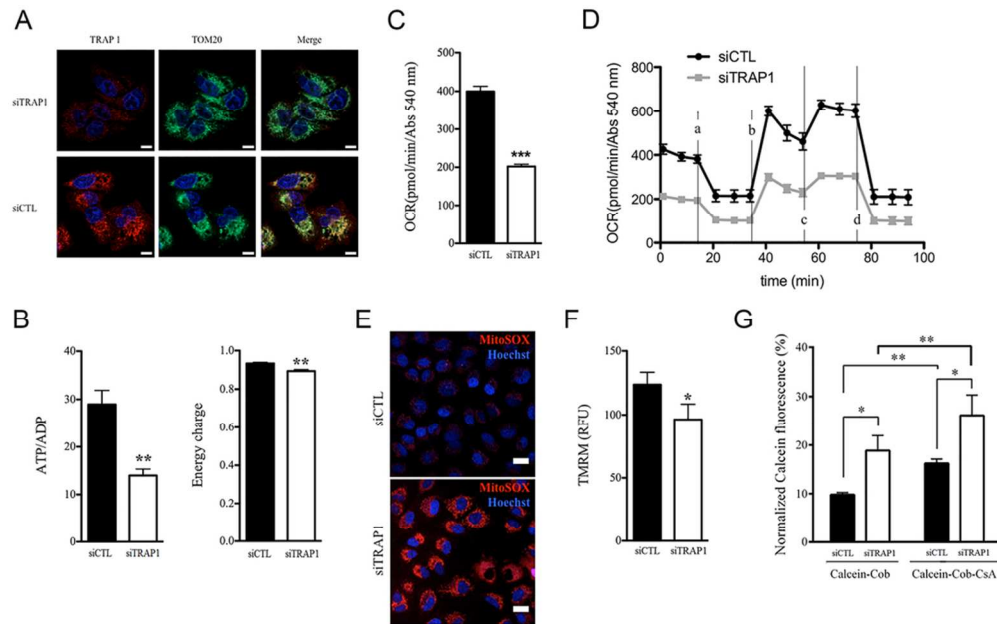


Figure 1. TRAP1 silencing results in mitochondrial dysfunction. (A) Confocal images illustrate siTRAP1 and siCTL cells labeled with anti-TOM20 and anti-TRAP1 antibodies to determine TOM20 and TRAP1 co-localization. DAPI labels nuclei. Scale bar = 8  $\mu$ m. (B) ATP, ADP and AMP measurements taken by HPLC indicate a decreased ATP/ADP ratio and energy charge in siTRAP1 cells. (C) Basal oxygen consumption measured with a Seahorse XFe96 Extracellular Flux Analyzer and displayed as oxygen consumption rate (OCR) is higher in siCTL than in siTRAP1 cells. Data are means  $\pm$  SEM from  $n = 3$  experiments. (D) Measurement of oxygen consumption rate (OCR) in both types of A549 cells using Seahorse Biosciences assay plates shows decreased respiration in siTRAP1 cells. Graphs are representative of three independent experiments and show the effects of mitochondrial inhibitors, (a) Oligomycin (2.5  $\mu$ M), (b) and (c) FCCP (500 nM) and (d) antimycin A (2.5  $\mu$ M) plus rotenone (2.5  $\mu$ M) injected as indicated. (E) Images of MitoSOX fluorescence in siTRAP1 and siCTL cells show an increase in mitochondrial superoxide anion production in siTRAP1 cells. Scale bar = 8  $\mu$ m. (F) TMRM fluorescence measured by flow cytometry reveals a lower mitochondrial membrane potential in siTRAP1 cells. Data are shown as relative fluorescence units (RFU) that represent the mean average of geometric mean values  $\pm$  SEM from three independent experiments. (G) Flow cytometric measurement of cobalt quenching of calcein fluorescence as an end-point for mPTP opening reveal a more closed conformation in siTRAP1 than in siCTL cells. Cyclosporin A (2  $\mu$ M) was able to close the pore in both types of A549 cells. Data are shown as relative fluorescence units (RFU) that represent the mean average of geometric mean values  $\pm$  SEM, normalized to fluorescence of cells incubated with calcein only for  $n=3$ . \* $p < 0.05$ ; \*\* $p < 0.01$ ; \*\*\* $p < 0.001$  vs. siCTL cells.

91x57mm (300 x 300 DPI)

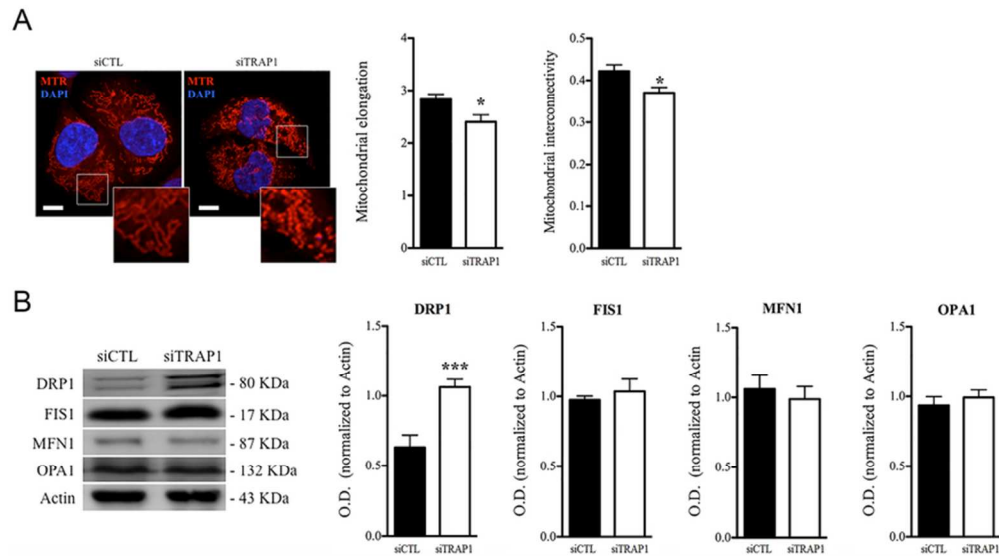


Figure 2 - TRAP1 silencing results in mitochondrial fragmentation. (A) Confocal images obtained using MitoTracker Red (MTR) for mitochondrial labeling and DAPI for nuclear labeling show alterations in mitochondrial morphology between siCTL and siTRAP1 A549 cells. Bar charts show mitochondrial elongation and interconnectivity measured using Image J in fluorescent images of siCTL and siTRAP1 cells stained with MTR. Data show mean  $\pm$  SEM from three separate experiments (15 cells per experimental condition and experiment). (B) Levels of proteins involved in mitochondrial dynamics (DRP1, FIS1, MFN1 and OPA1) indicate the occurrence of mitochondrial fission in siTRAP1 cells. Bar charts show means of optical density (O.D.)  $\pm$  SEM normalized to actin, from at least three separate immunoblots. \* $p < 0.05$ ; \*\*\*  $p < 0.001$  vs. siCTL cells.

73x40mm (300 x 300 DPI)

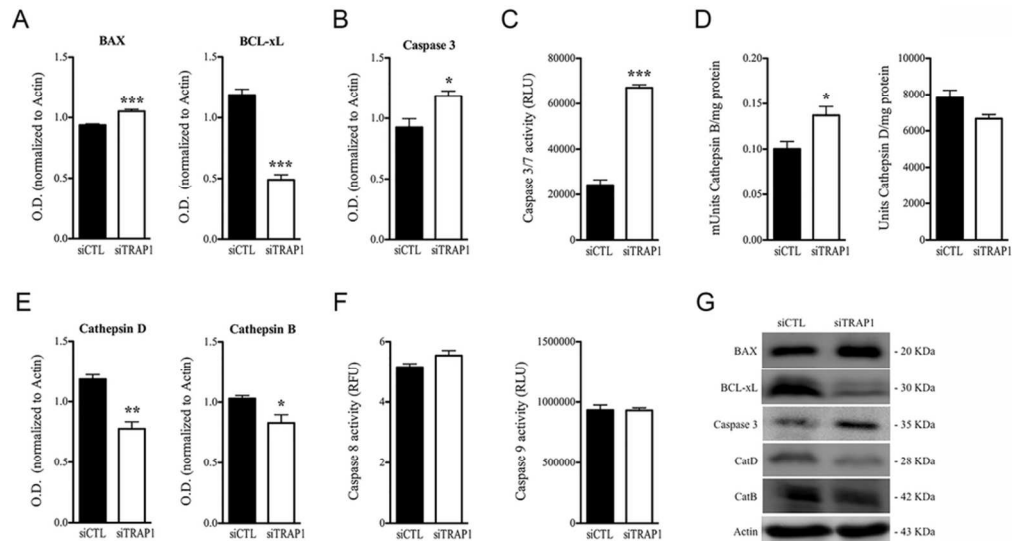


Figure 3. TRAP1 silencing alters cell death machinery. Expression of proteins involved in cell death (A) BAX, BCL-xL, and (B) caspase-3 indicates alterations in apoptotic pathways in A549 cells transfected with a TRAP1 siRNA (siTRAP1) in comparison with A549 cells transfected with a scrambled siRNA (siCTL). Bar charts show means of optical density (O.D.)  $\pm$  SEM normalized to actin, from at least three separate immunoblots. (C) Caspase 3/7-like activity showed an over-activation of caspase 3/7-like activity in siTRAP1 cells. (D) Cathepsin D and B activities were determined to test the activation of lysosomal processes of cell death, showing cathepsin B activation in siTRAP1 cells. Data are means of enzymatic units per mg of protein  $\pm$  SEM, from at least five independent experiments. (E) Immunoblot analysis against cathepsin D and cathepsin B shows decreased expression of both proteases upon TRAP1 silencing. (F) Caspases 8-, 9-like activities determined in both types of A549 cells showed no alterations in the initiator caspases. (G) Representative western blots. Data are expressed as means  $\pm$  SEM from at least three independent experiments. Bar charts show means of optical density (O.D.)  $\pm$  SEM normalized to actin, from at least three separate immunoblots. \*  $p < 0.05$ ; \*\*  $p < 0.01$ ; \*\*\*  $p < 0.001$  vs. siCTL cells.

83x45mm (300 x 300 DPI)

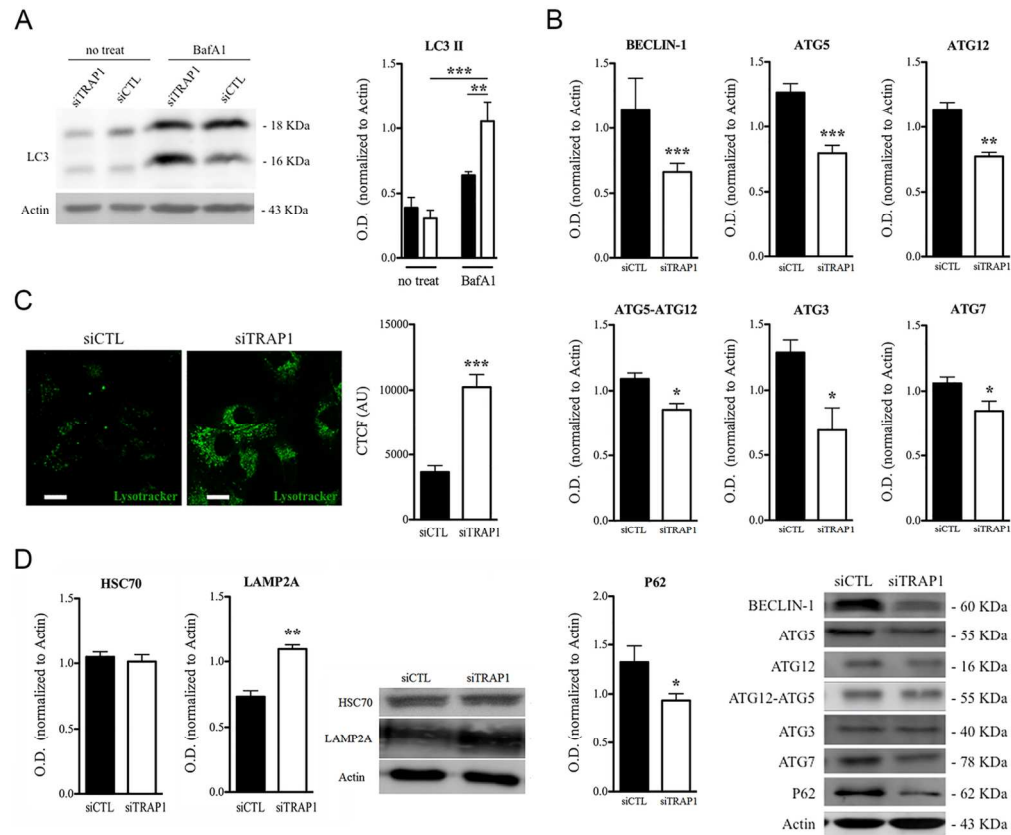


Figure 4. TRAP1 silencing activates macroautophagy. (A) LC3 protein expression analysis reveals no alterations in the amount of the marker of autophagosomes LC3-II between both types of A549 cells. To evaluate autophagic flux, both types of cells were treated with bafilomycin A (BafA1) showing a higher accumulation of LC3-II in siTRAP1 cells. Bar charts show means of optical density (O.D.)  $\pm$  SEM normalized to actin, from at least three separate immunoblots. (B) Immunoblot analysis against the autophagy-related proteins BECLIN-1, ATG5, ATG12, ATG3 and ATG7 suggests a down-regulation in the autophagic machinery in A549 cells transfected with a TRAP1 siRNA (siTRAP1) in comparison with A549 cells transfected with a scrambled siRNA (siCTL). However, p62 expression was lower in siTRAP1 cells indicating that autophagic flux is higher in TRAP1-silenced cells. (C) Labelling of acidic compartments using LysoTracker Green reveals the development of acidic organelles after TRAP1 silencing. Histogram shows means of corrected total cell fluorescence  $\pm$  SEM from three independent experiments (15 cells per experimental condition and experiment). (D) Protein expression of HSC70 shows no changes after TRAP1 depletion but LAMP-2A receptor shows a higher protein expression in siTRAP1 cells. Bar charts show means of optical density (O.D.)  $\pm$  SEM normalized to actin, from at least three separate immunoblots. \*  $p < 0.05$ ; \*\*  $p < 0.01$ ; \*\*\*  $p < 0.001$  vs. siCTL cells.

120x100mm (300 x 300 DPI)

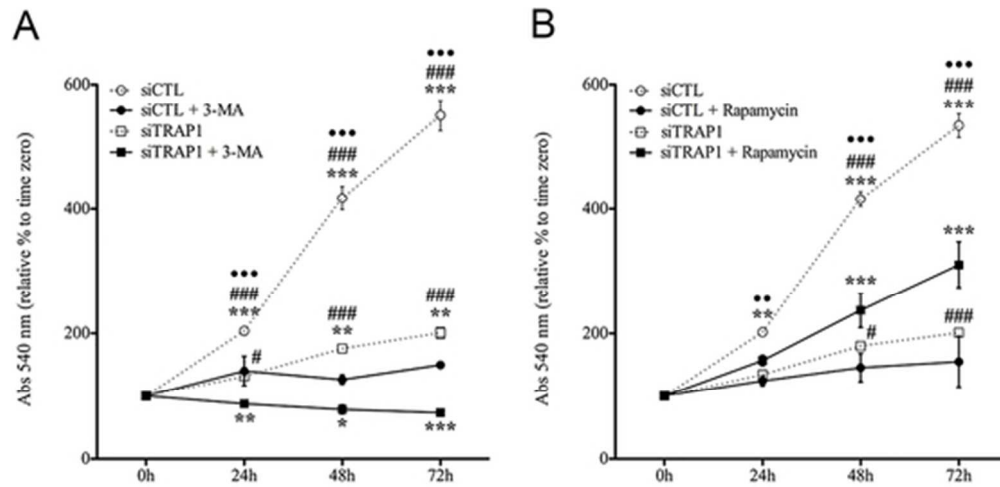


Figure 5. Effect of the autophagic drugs, (A) 3-methyladenine (3-MA, 5 mM), and (B) rapamycin (100 nM), on cell viability. Rapamycin increased the proliferation of siTRAP1. Data are expressed as percentage of the control (vehicle only) for each time point. Data are means  $\pm$  SEM from n=5. # Represents comparison with siTRAP1 cells treated with either rapamycin or 3-MA, \* represents comparison with siTRAP1 cells, and  $\square$  represents comparison with siCTL cells treated either with rapamycin or 3-MA.

46x22mm (300 x 300 DPI)